Electronic Supplementary Material (ESI) for RSC Applied Interfaces.

Supporting Information:

Characterizing Catalyst Function and Transformations in the Plasma Reduction of CO_2 on Atomic Layer Deposition-Synthesized Catalysts

Samuel K. Conlin,[1] Hamed Mehrabi,[2] David N. Parette,[1] Eva M. Nichols,[3] and Robert H. Coridan[1,2*]

[1] Department of Chemistry and Biochemistry, University of Arkansas, Fayetteville, AR, 72701, USA.

[2] Materials Science and Engineering Program, University of Arkansas, Fayetteville, AR, 72701, USA.

[3] Department of Chemistry, University of British Columbia, Vancouver, British Columbia, V6T 1Z4, Canada

*Email: rcoridan@uark.edu

Atomic Layer Deposition Parameters for the Growth of Al_2O_3, TiO_2, and ZnO on Aluminum-Silicate Fiber Support.

A base layer of Al_2O_3 was grown on the support from trimethylaluminum (TMA, 98%, Strem Inc.) and H_2O (HPLC grade, VWR Analytical) in an ALD reactor (GEMstar XT; Arradience Inc.). A thin base layer of Al_2O_3 was deposited onto the support to regularize the surface for catalyst deposition. Then the catalyst layer was deposited during the same ALD process utilizing a precursor corresponding to the catalyst layer and water as the oxidant. All thin films were deposited under a constant N_2 (99.999%; Airgas) flow of 20 sccm, metered by a mass flow controller with at 390 mTorr base pressure in the reactor. To deposit the base Al_2O_3 layer, the supports were placed inside the ALD chamber at 130 ˚C and exposed to 50 cycles of TMA and H_2O under N_2 flow (20 sccm) with room temperature precursor bottles. Each cycle consisted of an exposure to TMA, with precursor exposure controlled by valve-open time with constant N_2 flow (50 ms), a (chamber evacuating) purge step (45 s), then subsequent exposure to H_2O (21 ms) and another purge step (45 s). The Al_2O_3 samples were coated with an additional 93 cycles of TMA as previously described. The ZnO samples were prepared by deposition of the initial 50 cycles of TMA followed by 58 cycles of ZnO deposition from a diethylzinc precursor (DEZ, Strem Inc). Each ZnO deposition cycle consisted of an exposure to DEZ (50 ms), a purge step (45 s), then an exposure to H_2O (21 ms), and another purge step (45 s). The TiO_2 samples were prepared by deposition of the initial 50 cycles of TMA followed by 200 cycles of TiO_2 deposition with a tetrakis(dimethylamido)titanium precursor (TDMAT, 99%, Strem Inc). Each cycle of TiO_2 deposition consisted of an exposure to TDMAT (250 ms, 75 ˚C precursor temperature), a purge step (45 s), then an exposure to H_2O (21 ms pulse), and another purge step (45 s).

X-ray Photoelectron Spectroscopy (XPS) of Pre and Post DBD Plasma Exposed ALD-MOx Catalysts on Aluminum-Silicate Fiber Support.

Samples of ALD-MOx catalysts for XPS were prepared both before and after plasma exposure by removing small sample fibers from the interior of the support and placing them on a sample holder via conductive carbon tape. This holder was then stored in room air for 24 hours prior to measurement. The data was collected with with PHI Versaprobe Tetra XPS and analyzed using the CasaXPS software suite. Background subtraction was performed using the CasaXPS default sigmoidal-type *Shirley* method around the region of interest. Peak fitting was perfomed using the CasaXPS *Marquardt* peak type, and automatic fitting refinement was performed iteratively until the residual standard deviation from the measured data was minimized with the minimum number of peaks included. The absolute energy of each spectra was reference to the match the main feature position in the fresh, pre-plasma peak. While the C 1s position is generally used as a standard for calibrating binding energies in the scans, the C 1s feature intensity showed significant variability in position and intensity. This made it an obviously unreliable standard.

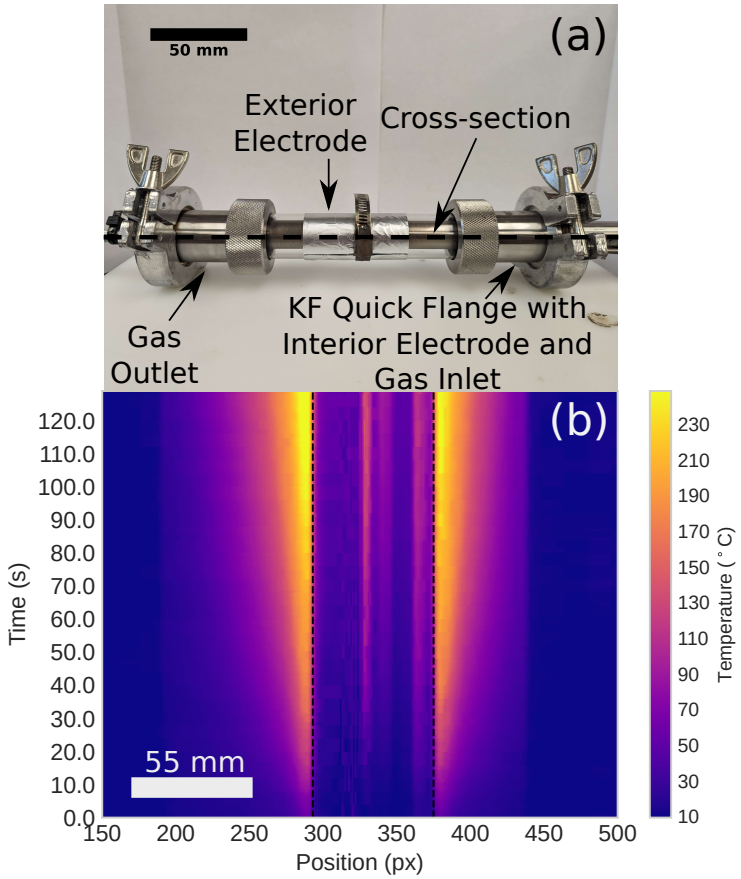

Figure S1 – (a) An image of the reactor setup, sans protective shielding. Arrows indicate the gas inlet and interior electrode mounted into a KF flange, the foil exterior electrode, and the gas outlet built into a KF flange. A dashed line also indicates the reactor cross section shown in Figure S1b below. (b) A waterfall plot showing the cross-sectional temperature of the outside of the reactor over a two-minute plasma reaction, as recorded by an infrared camera. The waterfall plot shows that the temperature of the uncooled reactor reached approximately 230 ˚C during the plasma reaction and was not uniform across the reactor body. The temperature was measured by taking the luminosity values of a 1x500 pixel stripe of every frame and comparing them against the luminosity of a linear temperature scale embedded in each image frame. The center of the reaction was blocked by the outer electrode, so the temperature at the center of the reaction volume was not measurable.

Equations for the Determination of CO_2 Conversion and Reactor Efficiency using ALD Catalysts on Regularized Supports from On-Line Gas Chromatograph Data

$$\text{Equation S1: } X_{CO_2} = 1 - \frac{n_{DBD}}{n_0}$$

Equation S1 describes the raw measurement of CO_2 converted (X_{CO_2}) into CO and O_2 from gas chromatography. It is calculated from gas chromatography measurements of the number of moles of CO_2 sampled during a 2-minute dielectric breakdown discharge (DBD) plasma reaction (n_{DBD}) and the number of moles of CO_2 sampled from flow through the reactor at the same flow rate without plasma (n_0).

$$\text{Equation S2: } f_{CO_2} = \frac{2X_{CO_2}}{3-X_{CO_2}}$$

Equation S2 describes the calculation of the total yield of converted CO_2, f_{CO_2}. The measured conversion fraction, X_{CO_2}, must be corrected for the constant pressure volumetric expansion due to the CO_2 splitting reaction, in which the stoichiometry indicates that two CO_2 molecules are split into three molecules:

$$\text{Reaction 1: } CO_2(g) \rightarrow \frac{1}{2}O_2(g) + CO(g) \qquad \Delta G^0_{rxn} = 257.2\ kJ\ mol^{-1}$$

This increase in the number of molecules increases the overall outlet flow rate and pressure, which must be compensated for due to calibrations being made at a constant gas flow and pressure of 1 atm

$$\text{Equation S3: } SEI = \frac{Input\ Power}{CO_2\ Flow\ Rate} * 60\ \frac{s}{min}$$

Equation S3 was used to calculate the specific energy input (SEI) per volume of CO_2 reactor flow at 1 atm, in units of J L^{-1}. In the main text, input power was measured in W, and CO_2 flow rate was set by the mass flow controller at 0.075 L min^{-1}.

$$\text{Equation S4: } \eta_{CO_2} = \frac{-\Delta G_{rxn} * f_{CO_2}}{SEI * V_{mol}} * 100\%$$

Equation S4 is the definition of the power conversion efficiency of the DBD plasma reactor process, as determined by the ratio of the power output in the form of CO (g) to the input electrical power provided to the DBD plasma reactor. The output power of the reactor considers the Gibbs free energy of the oxidation (the reverse of Reaction 1) and the rate of production of the product CO (g). V_{mol} = 22.4 L mol^{-1} is the standard molar volume of the ideal gas at 1 atm.

$$\text{Equation S5: } Rate\ Ratio = 1 + \frac{R_{plasma\ catalysis} - R_{Plasma\ Only}}{R_{Bare\ Support} - R_{Plasma\ Only}}$$

Equation S5 is the adapted rate ratio Barboun et al., which describes the ratio of plasma catalysis rate as performed by the plasma-gas-ALD catalyst surface interactions sans the plasma-only

phase reactions to the reaction rate at the plasma-gas-support interface, sans the plasma-only phase reactions.[1] This allows for the comparison of each of the ALD catalysts relative to one another given a constant plasma-support enhancement effect. This subtraction assumes the thermal catalysis contribution at the temperature of interest is negligible.

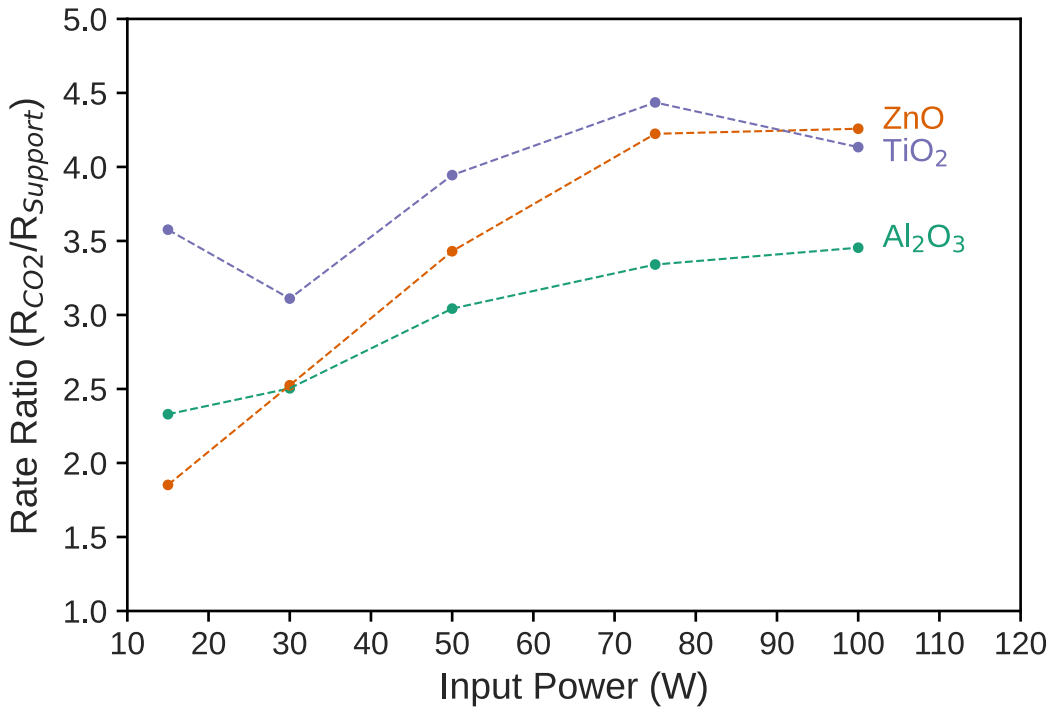

Figure S2- Rate ratio of the plasma-catalysis component rate ratio of the CO_2 conversion on each ALD catalyst to the bare support as a function of reactor input power. Each catalyst material was tested at a CO_2 flow rate of 75 sccm. The rate ratio of each point is derived from the average of the CO_2 conversion of each ALD catalyst at each input power.

Figure S2 is the derived rate ratios of the plasma catalysis contribution of the overall CO_2 conversion of each catalyst as compared to the bare support. The normalized packing and deposition of the ALD catalysts on the support coupled with the increasing rate ratios suggest that the activity of each support material is input power dependent, and the wide range of ZnO suggesting that it is the most variably active for CO_2 reduction, and at high powers demonstrates the greatest specific activity.

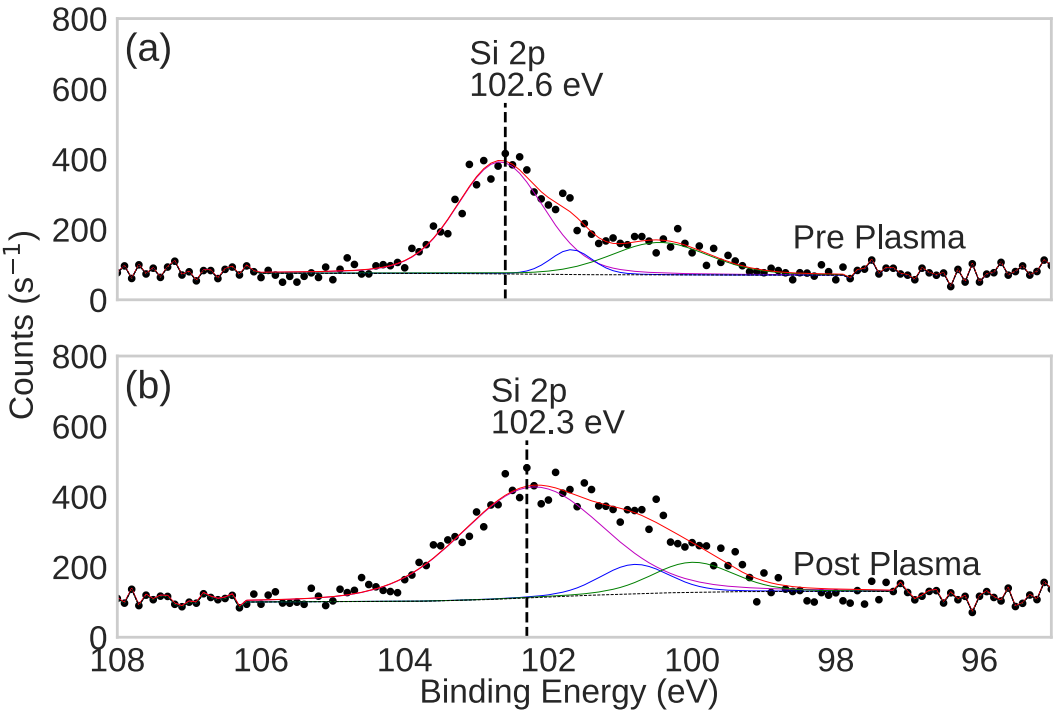

Figure S3 - XPS of Si 2p feature of the unmodified support (a) pre-plasma and (b) post-plasma catalysis. Solid lines indicate fitted features while the red dashed line indicates the sum of all fitted features. Dots indicate the counts as recorded and the dashed lower line indicates the fitted baseline.

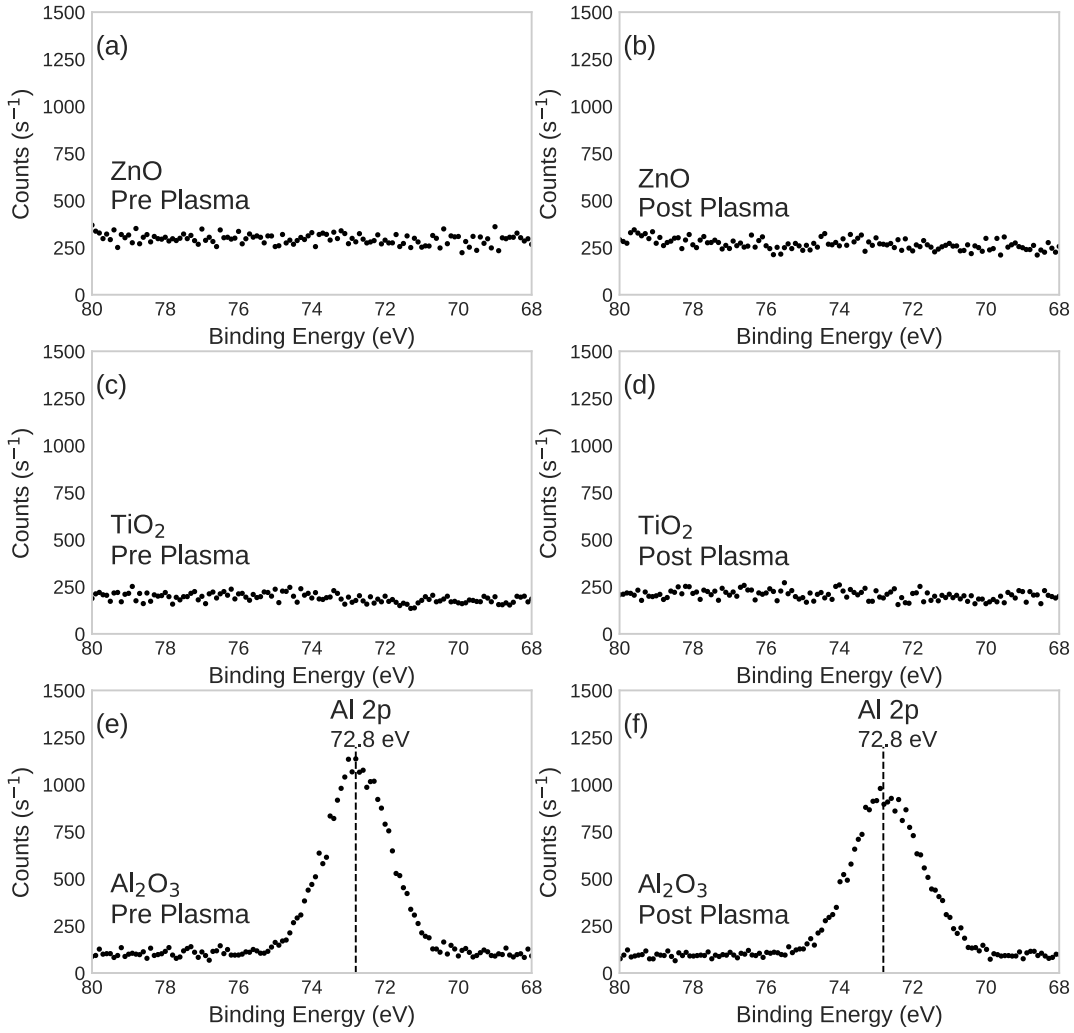

Figure S4 - XPS of Al 2p region of films pre and post catalysis. Black dots indicate the sum of signal collected during the sampling period.

Figure S4 is an array survey of the Al 2p region of the XPS spectrum of each of the ALD coated scaffolds before and after plasma exposure. The lack of a significant Al 2p feature from the underlying ALD Al_2O_3 layer in the TiO_2 and ZnO coated supports suggests that both catalysts maintained a conformal layer throughout the CO_2 plasma catalysis process for the times and input powers tested here.

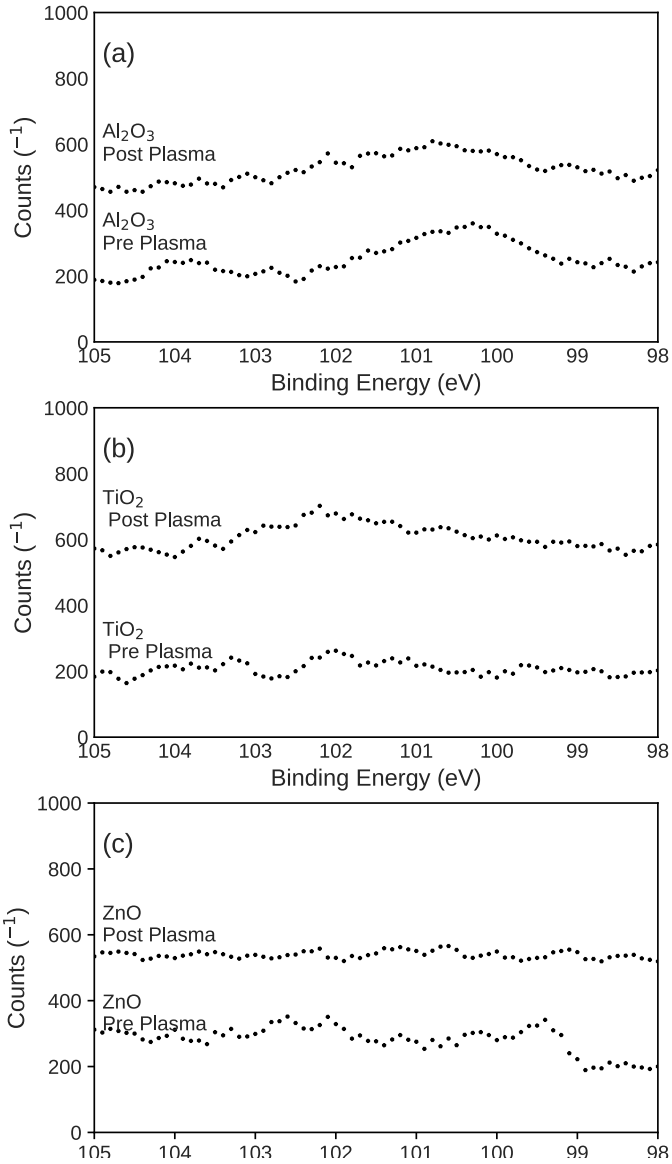

Figure S5 - XPS of Si 2p feature region of ALD catalyst pre-plasma and post-plasma exposure. Black dots indicate the sum of signal collected during the sampling period.

Figure S5 shows the Si 2p region of the ALD-coated supports before and after plasma exposure and indicates that the ALD Al_2O_3 base layers and ALD catalyst layers were deposited and remained intact throughout testing.

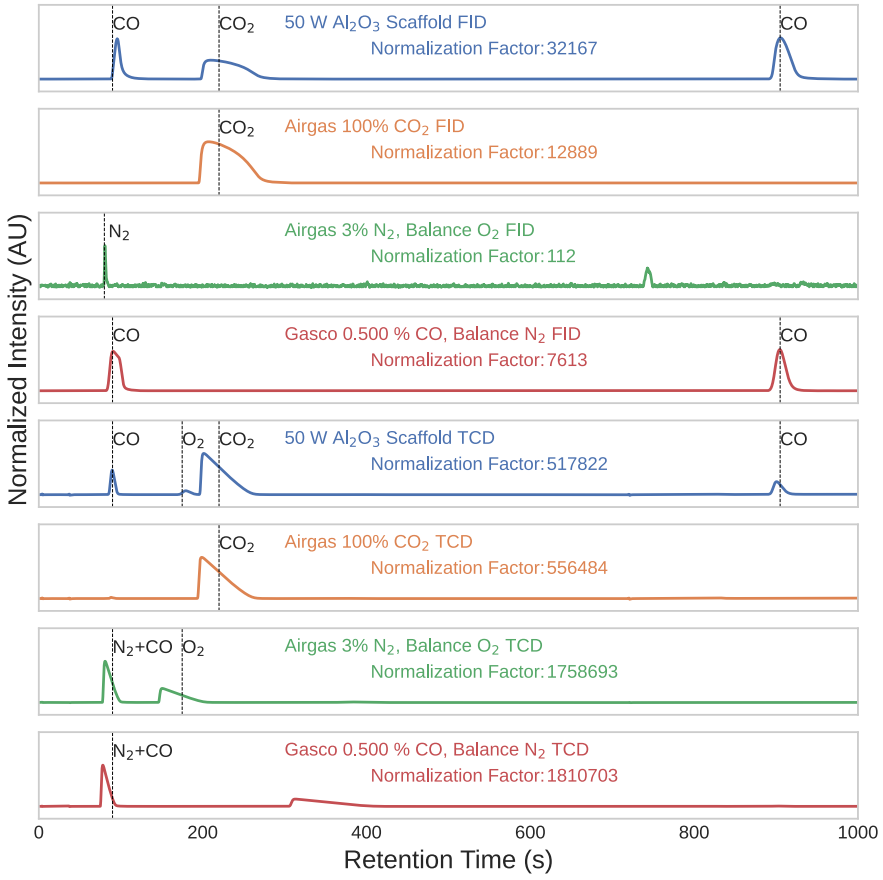

Figure S6 - Chromatograms of typical reactor output compared to known standards for peak matching and identification. Standard retention times for each molecular species and the overall intensity normalization factors for each measurement are shown for each chromatogram.

Figure S6 is an array of gas chromatograms used to show the retention time of the products of interest, primarily CO_2, CO, and O_2, under the same auto-sampling program as the experimental samples. Though we only used the consumption of CO_2 to indicate CO production, we show that we can distinguish between and are producing O_2 and CO from a 100% CO_2 input gas-stream. CO and N_2 are difficult to distinguish by retention time in the thermal conductivity detector (TCD) at a retention time of 80 s. The presence of CO can be verified unambiguously in the flame ionization detector (FID) during the second phase of the analytical GC procedure (retention time = 900 s).

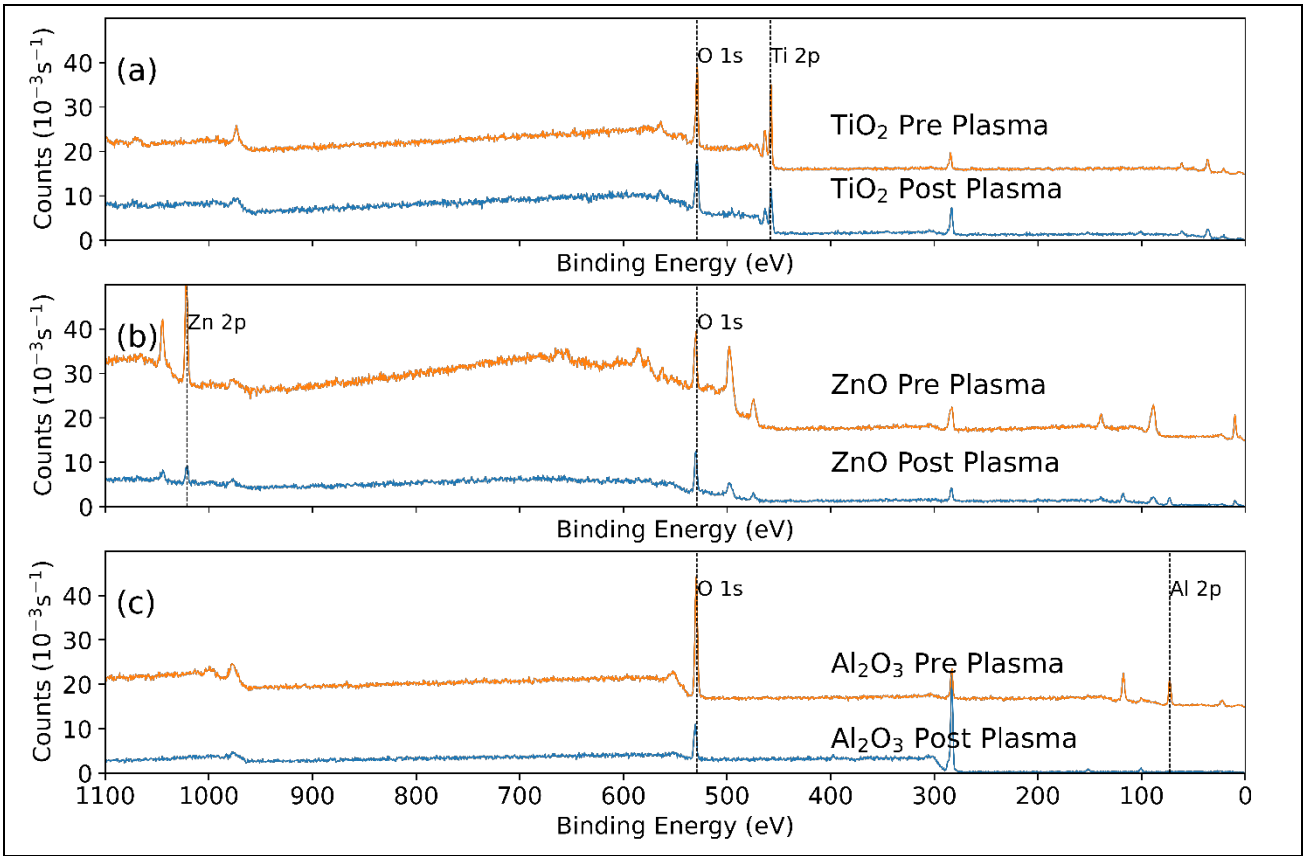

Figure S7- Survey XPS scans of the ALD-MOx catalyst pre and post plasma exposure. The orange (upper) line indicates the catalyst pre-plasma and the blue (lower) line indicates the catalyst post-plasma exposure. The spectra of the pre plasma catalyst have been vertically offset from the corresponding post plasma spectra for clarity.

Figure S7 is an array of survey XPS spectra of each of the ALD catalysts pre- and post-plasma exposure use to observe the presence or absence of the corresponding MOx before collecting more detailed, region-specific spectra. The relative intensities of the peaks of interest, the Ti 2p, Zn 2p, and Al 2p, can be seen in context with other signals such as the O 1s. The presence of the corresponding MOx on each catalyst can be seen both pre and post plasma, along with the lack of a major Si 2p peak component indicates that the catalyst survives plasma exposure intact and retains enough thickness as to not significantly expose the underlying silica.

References

(1) Barboun, P.; Mehta, P.; Herrera, F. A.; Go, D. B.; Schneider, W. F.; Hicks, J. C. Distinguishing Plasma Contributions to Catalyst Performance in Plasma-Assisted Ammonia Synthesis. *ACS Sustainable Chem. Eng.* **2019**, *7* (9), 8621–8630. https://doi.org/10.1021/acssuschemeng.9b00406.